Postprint. Mingcan Mei, Journal of Molecular Liquids, Volume 348 (2022) 118036
https://doi.org/10.1016/j.molliq.2021.118036

CO_2 capture by 1-ethyl-3-methylimidazolium acetate: solubility at low pressure and quantification of chemisorption and physisorption

Mingcan Mei,[1] Xutao Hu,[1] Zhen Song,[1] Lifang Chen,[1,*] Liyuan Deng,[2] and Zhiwen Qi[1,*]

[1] *State Key Laboratory of Chemical Engineering, School of Chemical Engineering, East China University of Science and Technology, 130 Meilong Road, 200237 Shanghai, China*

[2] *Department of Chemical Engineering, Norwegian University of Science and Technology, Sem Sælandsvei 4, 7491 Trondheim, Norway*

Corresponding authors: lchen@ecust.edu.cn (L.C.); zwqi@ecust.edu.cn (Z. Q.)

ABSTRACT: Although chemisorptive ionic liquids (ILs) are widely expected as promising CO_2 absorbents, rigorous thermodynamic analyses for such systems remain challenging due to the inevitable co-existence of chemisorption and physisorption. In this work, an experimental approach combining quantitative NMR (qNMR) spectroscopy and mass balance is proposed to straightforwardly quantify the chemisorption and physisorption of CO_2 in chemisorptive absorbent, and 1-ethyl-3-methylimidazolium acetate ([Emim][OAc]) is selected for an exemplary study. The total CO_2 solubility in [Emim][OAc] is measured by the pressure drop method, of which the chemisorption part is quantified by qNMR and the physisorption part is then determined by mass balance. Correspondingly, a large set of CO_2 solubilities at four temperatures (298.15 K, 313.15 K, 323.15 K, and 348.15 K) covering the low pressure range below 100 kPa are determined, where the chemisorption and physisorption contribution are distinguished quantitatively. Following that, thermodynamic analyses for the CO_2 absorption by [Emim][OAc] are made from chemisorption and physisorption point of view, respectively.

Keywords: CO_2 absorption, ionic liquids, chemi-physisorption, chemisorption and physisorption quantification, quantitative NMR

1. Introduction

Carbon dioxide (CO_2) capture and storage (CCS) is considered as one of the most common and cost-effective strategies to alleviate the increasingly severe greenhouse effect [1,2,3]. The current technology for CO_2 absorption in the industry mainly relies on aqueous alkanolamine solutions, e.g., monoethanolamine (MEA), 2-(diethylamino)ethanol (DEEA), and 3-(methylamino)propylamine (MAPA) through chemisorption [4,5]. However, such processes are unfavorably accompanied with corrosion, high energy consumption, and solvent loss [6,7]. To overcome these problems, ionic liquids (ILs) have been widely considered as alternative solvents for CO_2 absorption due to their unique properties such as negligible vapor pressure, high chemical and thermal stability, flexible designability, etc [8-14]. Chemisorptive ILs have been identified as optimal CO_2 absorbents due to its highly efficient absorption and activation capacity of CO_2 [8]. The phosphonium ILs [15,16], amino-based ILs [17-19] and imidazolium ILs [20-22] have been currently studied as common families in the field of CO_2 capture and storage.

Generally, phosphonium ILs with large relative molecular weight cause relative small molality for CO_2 solubility. For example, CO_2 solubility in trihexyl(tetradecyl)-phosphonium pyrazole ([P_{66614}][Pyr]) is 1.834 mol·kg^{-1} (1.02 mol·CO_2 mol^{-1} IL) at 296.15 K [15], while 1-ethyl-3-methylimidazolium acetate ([Emim][OAc]) is 2.138 mol·kg^{-1} (0.364 mol·CO_2 mol^{-1} IL) at 298.15 K [20]. For amino-based ILs, in spite of relatively high CO_2 absorption capacity, the introduction of amine groups results in high viscosity, and even more the viscosity of ILs dramatically increase by forming highly viscous glassy or gel-like materials after absorption of CO_2 [8,18]. Moreover, the enthalpy of CO_2 absorption in amino-based ILs is nearly -80 kJ·mol^{-1}, which means

that higher CO_2 capacity is achieved at the expense of higher enthalpy and energy consumption [8]. For imidazolium ILs, they have been widely studied because of simple structures, known absorption mechanism and activation capacity of CO_2 [22]. Nevertheless, the suitability of different ILs vary significantly from case to case due to remarkable differences in IL properties, especially the solubility for CO_2 [23]. Therefore, when evaluating a specific IL for CO_2 capture, it is a primary imperative to know its solubility for CO_2 in a wide temperature and pressure range.

In addition to the magnitude of CO_2 solubility, it is also highly desirable that the solubility behaviors of CO_2 in an absorbent could be revealed in more detail. For instance, one should examine whether the absorption process is physically or chemically based, and in case of chemisorption which also inevitably incorporates physisorption to a certain degree (could be essentially termed as chemi-physisorption) [24-26], the individual contribution of each should be recognized for clear thermodynamic analyses. Specifically, when considering the chemi-physisorption as a possible way to activate CO_2 for its further conversion to value-added products (e.g., carboxylic acids, carbonates, carbamates, etc.) [22,27-29], the quantification of chemisorption and physisorption is particularly important as it is exactly the chemical part rather than the physical part that determines the nature and the maximum yield of the target product [27].

Despite the great significance of the quantification of chemical and physical contribution in chemi-physisorption, limited attention has been paid to this point in previous literature [30,31]. Some studies directly kept the same thermodynamic fitting method as in pure physisorption for chemi-physisorption, which leads to questionable estimation of thermodynamic properties. For instance, Blath et al. [30] used Henry's law to fit the CO_2 solubility in [Emim][OAc] (a well-known chemical absorbent for

CO_2) under different temperatures and then derived the absorption enthalpy and entropy. Some studies (for example, Bishnoi et al. [31]) applied the N_2O analogy method to approximate the physical solubility of CO_2 in chemical absorbents by taking advantage of the non-reactivity and similarity to CO_2 in terms of configuration and molecular volume of N_2O. Nevertheless, this method not only requires repeated absorption experiment for CO_2 and N_2O, but also is restricted to a concentration and temperature range where the analogy holds [32]. Additionally, a few studies have indirectly fitted the Henry's law constant of physisorption and the equilibrium constant of chemisorption under the assumption of the chemical reaction mechanism [24,25,33]. In short, there is still no straightforward and easy approach for the accurate quantification of chemisorption and physisorption of CO_2 in reactive absorption systems.

Taken together the aforementioned aspects, this work proposes an experimental approach by combining quantitative NMR (qNMR) spectroscopy and mass balance for the clear distinction of the chemisorption and physisorption of CO_2 in chemi-physisorption systems. As a common chemisorptive IL, [Emim][OAc] has advantages of specific absorption product Emim-CO_2 adduct, simple structure, and appropriate characteristic peaks in ^{1}H NMR spectra before and after CO_2 absorption [21]. To exemplify the proposed method, [Emim][OAc] is taken as a representative chemical absorbent. A large set of CO_2 solubilities in this IL are measured experimentally within the pressure range below 100 kPa at four different temperatures (298.15 K, 313.15 K, 323.15 K, and 348.15 K). By employing the proposed method, the physical and chemical contribution in the measured CO_2 solubility are quantified, following which thermodynamic analyses for the CO_2 absorption by [Emim][OAc] are made rationally.

2. Method

2.1. Materials

CO_2 with a mole fraction of 0.9999 was supplied by the Shanghai Wetry Standard Reference Gas Co., Ltd., China. The ionic liquid [Emim][OAc] (98%) was purchased from the Lanzhou Institute of Chemical Physics, China. The internal standard of NMR, 3,4,5-trichloropyridine (> 98%), was purchased from the Shanghai Titan Scientific, China. Acetic acid (HOAc, ≥ 99.8%) were purchased from the Shanghai Aladdin Biochemical Technology Co., China. The NMR solvent dimethyl sulfoxide-d_6 (DMSO-d_6, 99.9%) was purchased from Cambridge Isotope Laboratories, America. All chemicals were utilized as received without further purification unless otherwise specified. Notably, the purchased [Emim][OAc] was measured immediately through Hiranuma AQV-300 Karl Fischer titration and the average water content is 0.17 wt% after three tests. Then, it was protected with N_2 and stored in a desiccator with molecular sieve to prevent adsorption of water. Afterwards, [Emim][OAc] was degassed and dried at 333.15 K through rotary evaporation under vacuum at least for 24 h before each absorption experiment.

2.2. Proposed quantification method

The proposed method for the quantification of chemisorption and physisorption in chemi-physisorptive system is shown in Fig. 1, which consists of three steps:

Step I. The total absorption capacity (C_{CO2}) for CO_2 is first measured by the system pressure drop method, which will be introduced in Section 2.3.

Step II. The chemisorption capacity (C_{chem}) is then determined by ^{1}H qNMR under optimized conditions, which will be detailed in Section 2.4.

Step III. The physisorption capacity (C_{phys}) is finally calculated by the mass

balance between C_{CO2}, C_{chem} and C_{phys}.

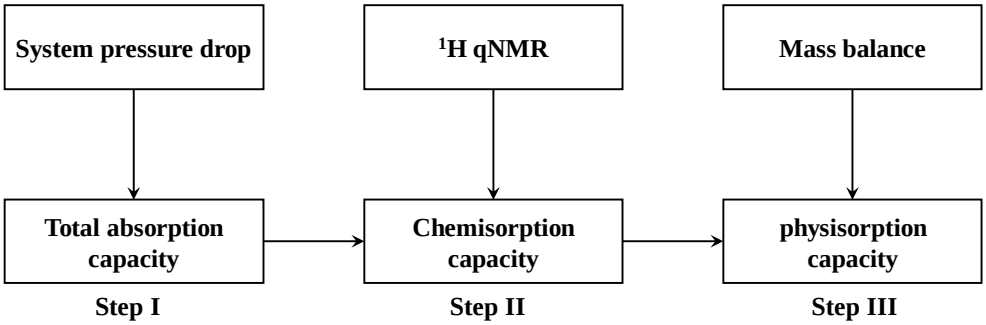

Fig. 1. Proposed method for quantifying chemisorption and physisorption.

The quantification of chemisorption and physisorption in a chemi-physisorptive process can be determined and should consider following conditions.

(1) The solvent must contain inactive hydrogen atoms (bonded to carbon atoms) in order to guarantee that the intensity of the response signal is proportional to the number of nuclei causing such particular resonances (Eq. (1)) [34]. For example, the exchangeable imidazolyl protons are not considered viable for ^{1}H qNMR.

$$I \propto N \tag{1}$$

where I refers to the integral signal area, N is the number of excited atoms in the molecule.

(2) The solvent should have simple and readily distinguishable characteristic peaks on the spectrum.

(3) The chemical absorption products by the reaction of absorbent and gas can be detected by NMR.

(4) The characteristic peaks of unreacted absorbent and reaction products do not interfere with each other.

2.3. Total CO_2 absorption

The absorption capacity of CO_2 was determined through the pressure drop method by using the apparatus illustrated in Fig. S1 (Supporting Information), as reported earlier by our group [35-37]. The apparatus mainly consists of a pressure transducer (Series 33X, Keller Co., Switzerland) with an accuracy of ±0.2 kPa, a gas reservoir (V_{GR} = 150±0.1 mL) and a gas absorption reactor (V_{AR} = 30±0.1 mL). After introducing a known amount of [Emim][OAc] (weighted on an electronic balance, Sartorius/Germany, ±0.0001 g), the system was controlled at the certain temperature T (298.15 K, 313.15 K, 323.15 K, and 348.15 K) and then was evacuated with a vacuum pump to a pressure of p_{inert}. The gas reservoir was charged to a pressure of p_1 by a gas cylinder with CO_2. The absorption was initiated after CO_2 entering into the absorption reactor with a magnetic stirrer (V_m = 1 mL) spinning around at 300 rpm, and the pressure in the system fell to p_2 shortly. The experiment was terminated when the pressure of p_3 remained constant for 1 h with continuous stirring. Due to the negligible vapor pressure of [Emim][OAc], the partial pressure of CO_2 in the gas reservoir as the feed (p_{feed}) and at equilibrium (p_{equ}) can be calculated as:

$$p_{feed} = p_1 - p_{inert} \quad (2)$$

$$p_{equ} = p_3 - p_{inert} \quad (3)$$

The solubility of CO_2 in [Emim][OAc] (n_{CO2}) can thus be derived as:

$$n_{CO2} = \rho_g(p_{feed}, T) \times V_{GR} - \rho_g(p_{equ}, T) \times V_{sys} \quad (4)$$

where $\rho_g(p, T)$ denotes the density of CO_2 in mol·cm^{-3} at T under pressure p obtained from the NIST Standard Reference Data; V_{sys} refers to the volume of the absorption system ($V_{GR} + V_{AR} - \frac{m_{IL}}{\rho_{IL}(T)} - V_m$), and $\rho_{IL}(T)$ is the density of [Emim][OAc] in g·cm^{-3} at T, which was measured by a digital density meter (DMA-4500 M, Anton Paar,

Austria). As the molar quantity of [Emim][OAc] (n_{IL}) is readily known from its mass weight and molecular weight, the mole absorption capacity (C_{CO2} in mol CO_2·mol^{-1} IL) and the molar fraction (x_{CO2}) of CO_2 in [Emim][OAc] can be attained by:

$$C_{CO2} = \frac{n_{CO2}}{n_{IL}} \tag{5}$$

$$x_{CO2} = \frac{n_{CO2}}{n_{IL} + n_{CO2}} \tag{6}$$

2.4. ^{1}H qNMR spectroscopy

A known mass of {[Emim][OAc] + CO_2} liquid mixture sample after CO_2 absorption and internal standard were dissolved in 0.6 mL DMSO-d_6 and then transferred to an NMR tube. ^{1}H NMR spectra were recorded at 298.15 K on a 600 MHz spectrometer (Avance Neo, China) using 5 mm probes. Chemical shifts (δ) were reported in parts per million (ppm) downfield from tetramethylsilane (TMS) and referenced to residual protium in a common aprotic solvent DMSO-d_6 (δ = 2.50 ppm). Notably, the chemisorptive product is particularly stable in DMSO-d_6 [38].

To quantify the NMR spectrum information, the relaxation delay ($d1$) and number of scans (Ns) need to be optimized to meet the relationship of Eq. (1). The $d1$ = 30 s and Ns = 16 were determined as the optimal parameters by investigating the change of peak area ratio of the sample to the internal standard with $d1$ and Ns (detailed in Fig. S2, Supporting Information). The other operation parameters (such as spectrometer frequency, spectral width, pulse width, receiver gain, and pulse angle) are relatively independent of the NMR equipment manufacturer, which were set to fixed values combined with the recommended values in literature [39,40]. Table 1 summarizes the quantitative NMR parameters used in this work.

Based on Eq. (1) and the optimal ^{1}H qNMR parameters, the molar ratio n_X/n_Y

between two compounds X and Y can be calculated as:

$$\frac{n_X}{n_Y} = \frac{I_X/N_X}{I_Y/N_Y} \tag{7}$$

Likewise, the fraction of compound X in a mixture of *Z* components can also be calculated as:

$$\frac{n_X}{\sum_{i=1}^{Z} n_i} = \frac{I_X / N_X}{\sum_{i=1}^{Z} I_i / N_i} \tag{8}$$

Table 1. ^{1}H qNMR experimental parameters.

Parameters	Values
Spectrometer frequency (MHz)	600.13
Spectral width (Hz)	11,904.8
Pulse width (s)	12
Receiver gain	11
Pulse angle (°)	30
Relaxation delay (*d*1)	30
Number of scans (*N*s)	16

2.5. Uncertainty calculation

The expanded uncertainty of the total absorption capacity of an absorbent for CO_2 ($U_c(C_{CO2})$) with a level of confidence of approximately 95% can be calculated as follows [35]:

$$\frac{u(n_i)}{R/n_i} = \sqrt{\left(\frac{u(p_i)}{p_i}\right)^2 + \left(\frac{u(V_i)}{V_i}\right)^2 + \left(\frac{u(T_i)}{T_i}\right)^2} \tag{9}$$

$$u(n_{IL}) = \frac{u(m)}{M} \tag{10}$$

$$\frac{u_c(C_{CO2})}{C_{CO2}} = \sqrt{\frac{(\sum u(n_i))^2}{n_g^2} + \frac{(u(n_{IL}))^2}{n_{IL}^2}} \tag{11}$$

$$U_c(C_{CO2}) = 2u_c(C_{CO2}) \tag{12}$$

where $u_c(C_{CO2})$ is the combined uncertainty of CO_2 total absorption capacity in solvent and R is the universal gas constant. The measurement uncertainties of pressure, volume, temperature, and mass are $u(p)$ = 0.2 kPa, $u(V)$ = 0.1 mL, $u(T)$ = 0.1 K, and $u(m)$ = 0.0001 g, respectively.

The expanded uncertainty of CO_2 chemisorption capacity ($U_c(C_{chem})$) [41] in solvent was calculated by:

$$u\left(\frac{I_{IL}}{I_{product}}\right) = \sqrt{\frac{\sum_{i=1}^{n}(x_i - \bar{x})^2}{n(n-1)}} \tag{13}$$

$$u_c\left(\frac{n_{IL}}{n_{product}}\right) = \frac{n_{IL}}{n_{product}}\sqrt{\left(\frac{u(I_{IL}/I_{product})}{I_{IL}/I_{product}}\right)^2} \tag{14}$$

$$U_c(C_{chem}) = 2u_c(C_{chem}) \tag{15}$$

where x_i represents the result of a single measurement i whereas $\bar{x}$ is the mean value of n measurements. I_{IL} and $I_{product}$ stand for the integral area of [Emim][OAc] and the chemisorptive product, respectively. The $u_c(n_{IL}/n_{product})$ is the combined uncertainty, which contains and describes all uncertainties and errors of the whole measurement procedure.

The expanded uncertainty of CO_2 physisorption capacity ($U_c(C_{phys})$) in solvent was calculated by Eqs. (16) and (17):

$$u_c(C_{phys}) = \sqrt{u_c^2(C_{CO2}) + u_c^2(C_{chem})} \tag{16}$$

$$U_c(C_{phys}) = 2u_c(C_{phys}) \tag{17}$$

3. Results and discussion

3.1. Validation of the pressure drop method

Although [Emim][OAc] has already been tested for the absorption and activation of CO_2 by several studies [20,22,42,43], it is surprising to find that its solubility for CO_2 is scarcely covered in the low pressure range. Therefore, this work first systematically measures a set of CO_2 solubilities in this IL within the low pressure range below 100 kPa at four different temperatures (298.15 K, 313.15 K, 323.15 K, and 348.15 K).

As shown in Fig. 2, in addition to the very few available data points in this pressure range in literature, totally 32 new data points (eight for each of the four temperatures) are measured in this work. Particularly, there are no CO_2 solubility data in this IL at 313.15 K in previous literature. Moreover, a very good agreement was found by comparing the newly measured CO_2 solubility data in this work with those previously available in literature [20,43]. In this sense, the pressure drop method employed for measuring the total CO_2 solubility is validated to be reliable.

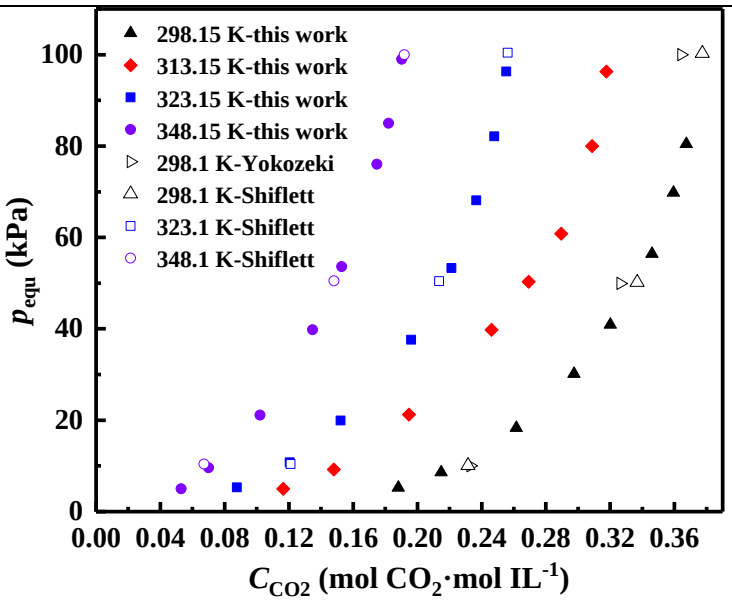

Fig. 2. Total solubility of CO_2 in [Emim][OAc] at low pressures below 100 kPa.

The Jou and Mather model [44] is generally used to fit CO_2 absorption in different systems and our group have also reported this mode for CO_2 absorption in imidazole-PTSA based deep eutectic solvents and mixed solvent system of alkanolamines and poly(ethylene glycol) [37,45]. The expression of the model is as follows:

$$\ln p_{equ} = A + B\ln C_{CO2} \tag{18}$$

$$A = a + bT + cT^2 \tag{19}$$

$$B = d + eT + fT^2 \tag{20}$$

where A and B are function of temperature. The coefficients are correlated and listed in Table 2, and calculated and experimental p_{CO2} are compared and illustrated in Fig. 3.

Table 2. Coefficients of correlations

Solution	Coefficients					
	a	b (K^{-1})	c (K^{-2})	d	e (K^{-1})	f (K^{-2})
[Emim][OAc]	76.6476	0.4272	6.6357E-4	110.6449	0.6353	9.3109E-4

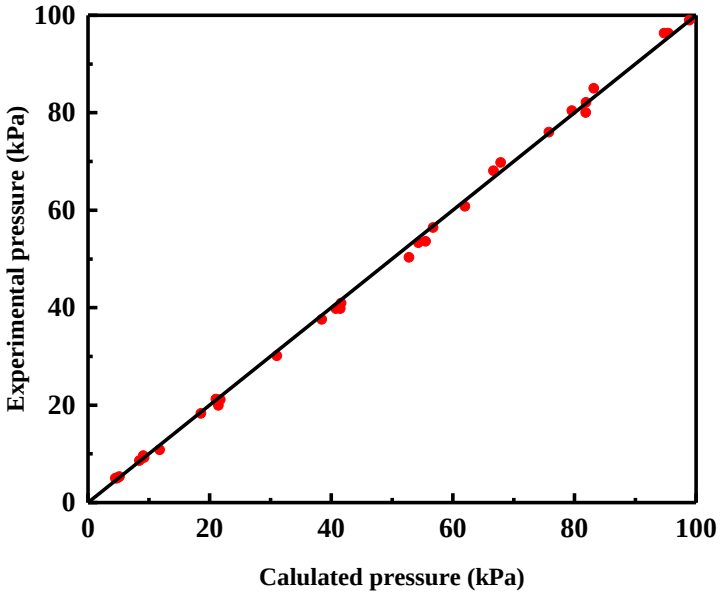

Fig. 3. The comparison between experimental and calculated CO_2 partial pressure.

The model deviation is indicated as average relative deviation (AARD) according to Eq. (21).

$$\mathrm{AARD} = \frac{1}{n} \times \sum_n \left| \frac{p_{\mathrm{CO2,exp}} - p_{\mathrm{CO2,cal}}}{p_{\mathrm{CO2,exp}}} \right| \times 100\% \tag{21}$$

where $p_{\mathrm{CO2,exp}}$ and $p_{\mathrm{CO2,cal}}$ refer to the partial CO_2 pressure of experiment and calculation, respectively; n is the total number of experiment data points. The experimental results agree well with calculated data by Jou and Mather empirical model, with a small AARD of 5.29%.

3.2. ^{1}H qNMR measurement validation

As the reliability of the pressure drop method for measuring the total CO_2 solubility is well proved, the following validates the feasibility and accuracy of the ^{1}H qNMR for the C_{chem} determination.

As already been clearly demonstrated, in the chemisorption of CO_2 by [Emim][OAc], CO_2 reacts with [Emim][OAc] in a stoichiometric ratio of 1:1 to form

Emim−CO_2 adduct (the chemisorptive product mentioned above) and HOAc [21,22] (see Scheme 1). Thus, the amount of Emim−CO_2 adduct can represent the C_{chem} of the {[Emim][OAc] + CO_2} system. Fig. 4 compares the ^{1}H NMR spectra of [Emim][OAc] before and after CO_2 absorption, where the new peaks appearing after the formation of Emim−CO_2 adduct are clearly independent of the peaks of the unreacted [Emim][OAc]. That is to say, the ^{1}H qNMR method on the amount of the in-situ formed Emim−CO_2 adduct offers a promising approach to determining C_{chem} in this system.

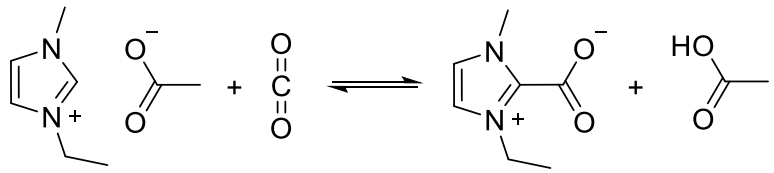

Scheme 1. Chemical reaction of CO_2 with [Emim][OAc].

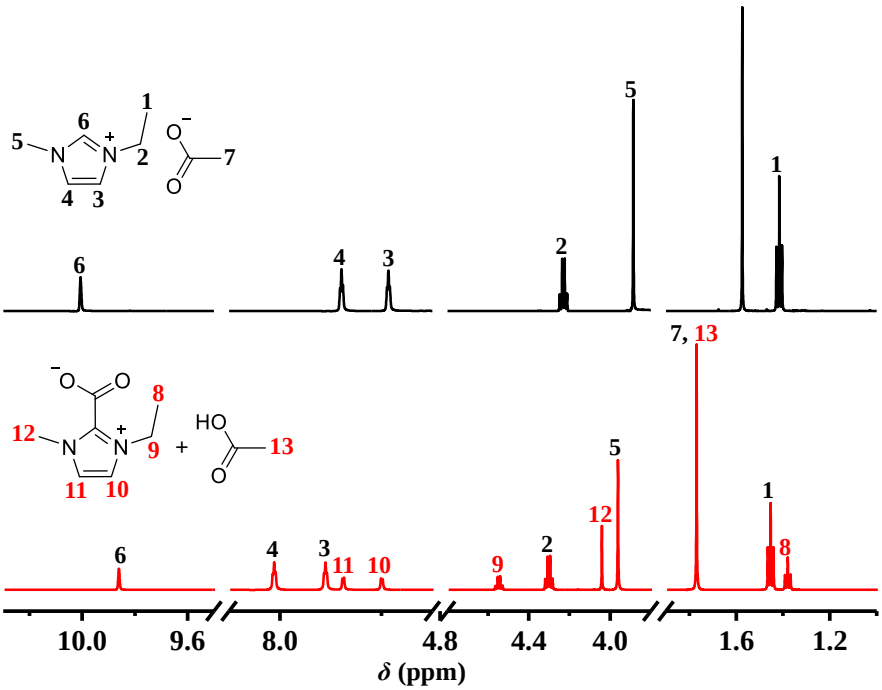

Fig. 4. ^{1}H NMR spectra of [Emim][OAc] before and after the capture of CO_2.

According to Eq. (1), the peak areas are the important data to obtain the amount of Emim−CO_2 adduct, while the discernible distance between the independent peak pairs (labeled by 1 and 8, 2 and 9, 3 and 10, 4 and 11, 5 and 12) of [Emim][OAc] and

Emim−CO_2 adduct (Fig. 4) is the preconditions to obtain integral area. As shown in the enlarged view (Fig. S3, Supporting Information), the methylene group in the ethyl side chain of [Emim][OAc] and Emim−CO_2 adduct (2 and 9 in Fig. S3b) are selected as a pair of characteristic peaks due to their proper chemical shift difference ($\Delta\delta = 0.25$ ppm) that can prevent the appearance of overlapping peaks from changing the sample concentration.

As the ratio of the integral area I to excited atoms N stands for the amount of a compound, C_{chem} can be simply expressed by Eq. (22) with the same excited atoms ($N_{IL} = N_{adduct} = 2$) in both [Emim][OAc] and Emim−CO_2 adduct.

$$C_{chem} = \frac{I_{adduct} / N_{adduct}}{I_{IL} / N_{IL} + I_{adduct} / N_{adduct}} = \frac{I_{adduct}}{I_{IL} + I_{adduct}} \quad (22)$$

where I_{IL} and I_{adduct} refer to the integral area of peaks 2 and 9, respectively, shown in the ^{1}H NMR spectrum of [Emim][OAc] after CO_2 capture (Fig. 4).

In order to verify the accuracy of ^{1}H qNMR, five model solutions were prepared that contain [Emim][OAc] and HOAc in different molar ratios (from 0.0096 to 0.5014) solved in DMSO-d_6, shown in Table S1 (Supporting Information). The molar ratios obtained by gravimetric reference significantly correlate ($R^2 = 0.9999$) with the those obtained by ^{1}H qNMR (Fig. 5), which indicated that ^{1}H qNMR has the capacity to reflect the actual content of substances with methylene group as the characteristic peak [40].

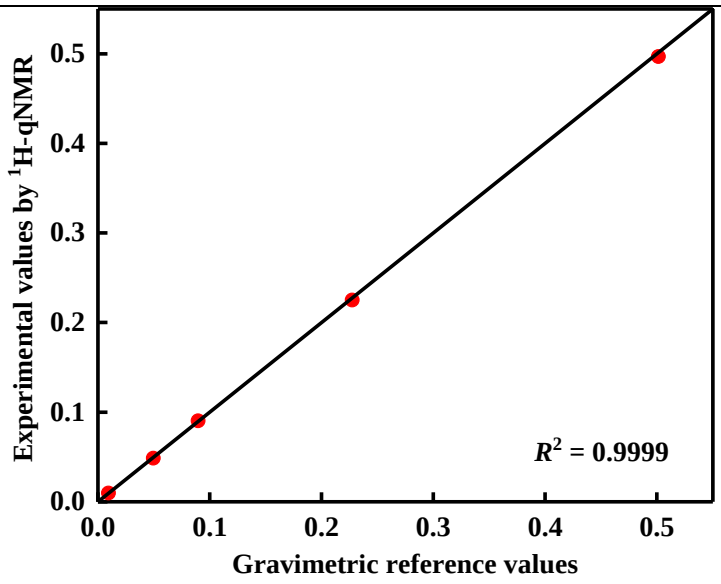

Fig. 5. Correlation between the molar ratios of [Emim][OAc] and HOAc quantified by using gravimetrical analysis and ^{1}H qNMR method.

3.3. Chemisorption and physisorption capacity of CO_2 in [Emim][OAc]

Based on the framework shown in Fig. 1, the total absorption capacity C_{CO2} in [Emim][OAc] is calculated by Eq. (4) when the {[Emim][OAc] + CO_2} system reaches equilibrium. 32 entries of C_{CO2} were measured at 298.15 K, 313.15 K, 323.15 K and 348.15 K and an equilibrium pressure below 100 kPa (Fig. 2). The amount of Emim−CO_2 adduct of each entry is measured by the developed ^{1}H qNMR method to accurately determine C_{chem} (see the corresponding ^{1}H qNMR spectra in Figs. S4-S7, Supporting Information), and following that, C_{phys} is determined according to mass balance.

To prove that the structure of Emim−CO_2 adduct will not be destroyed during the sample preparation process, the operation conditions that may affect the ^{1}H qNMR results were explored, including the effect of NMR solvent, pressure and temperature. The results were shown in Supporting Information S3, which verifies that the absorption equilibrium will not be affected during the sample preparation process

[22,26]. The obtained C_{chem} and C_{phys} of 32 entries are illustrated in Fig. 6 with the detailed data as well as the results of error analysis in Table S2 (Supporting Information). Taking the absorption at 298.15 K and 8.6 kPa as an example as shown in Fig. S4b, the integral areas of quantitative peak pairs are 25.04 and 5.96 for [Emim][OAc] and Emim−CO_2 adduct, respectively. Therefore, according to Eq. (22) and Step III (Section 2.2), C_{chem} and C_{phys} under such conditions are 0.1923 and 0.0226 mol·CO_2 mol^{-1} IL, respectively.

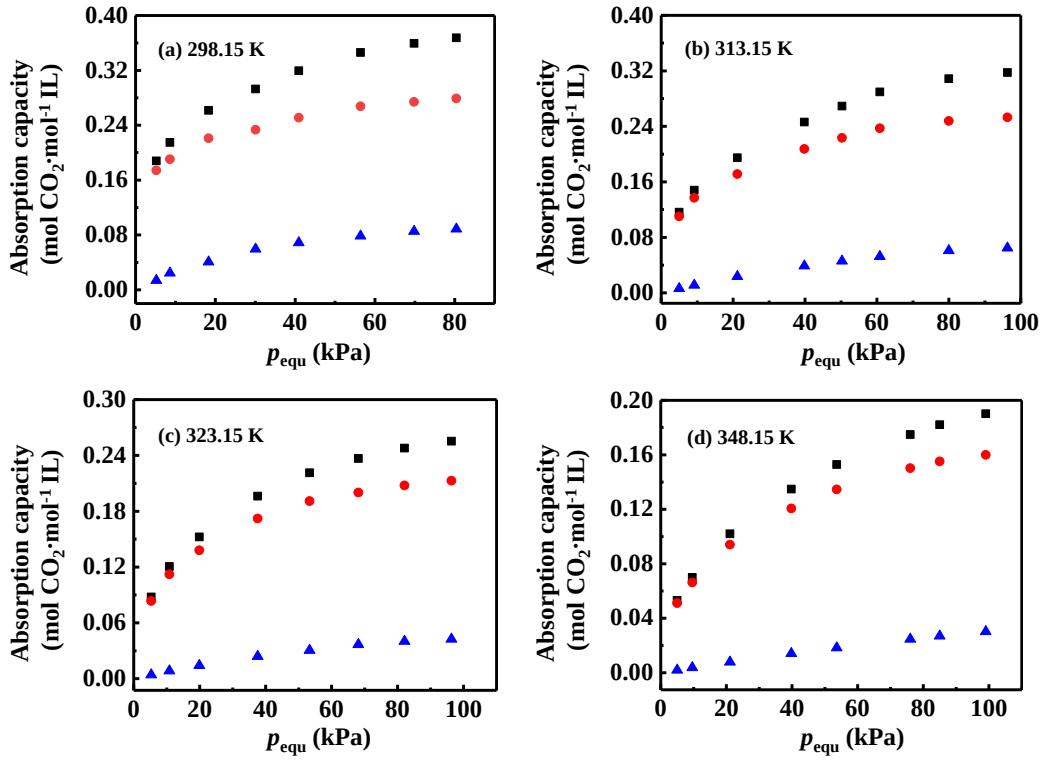

Fig. 6. Absorption capacity of CO_2 in [Emim][OAc] under equilibrium pressure of 0 kPa to 100 kPa at (a) 298.15 K, (b) 313.15 K, (c) 323.15 K and (d) 348.15 K. ■ total absorption capacity (C_{CO2}); ● chemisorption capacity (C_{chem}); ▲ physisorption capacity (C_{phys}).

From Fig. 6, the equilibrium pressure has a positive influence on C_{CO2}, C_{chem}, and C_{phys}. When it is raised from 10.8 kPa to 96.3 kPa at a given temperature (e.g., 323.15

K in Fig. 5c), C_{CO2}, C_{chem}, and C_{phys} increase from 0.1205, 0.1123, and 0.0082 mol CO_2·mol^{-1} IL to 0.2553, 0.2119, and 0.0434 mol CO_2·mol^{-1} IL, respectively. In comparison, the temperature has a negative influence. When it is raised from 313.15 K to 323.15 K (Fig. 5b and 5c), C_{CO2}, C_{chem}, and C_{phys} decrease from 0.3177, 0.2530, and 0.0647 mol CO_2·mol^{-1} IL to 0.2553, 0.2119, and 0.0434 mol CO_2·mol^{-1} IL under 96.3 kPa, respectively.

Fig. 6 also implies that the contribution of chemisorption and physisorption to absorption process is affected by temperature and pressure. In order to clearly describe the phenomenon, the absorption capacity was further analyzed as illustrated in Fig. 7. Among them, the data of Fig. 7b refers to the ratio of the chemisorption and physisorption (α) as calculated by Eq. (23).

$$\alpha = \frac{C_{chem}}{C_{phys}} \tag{23}$$

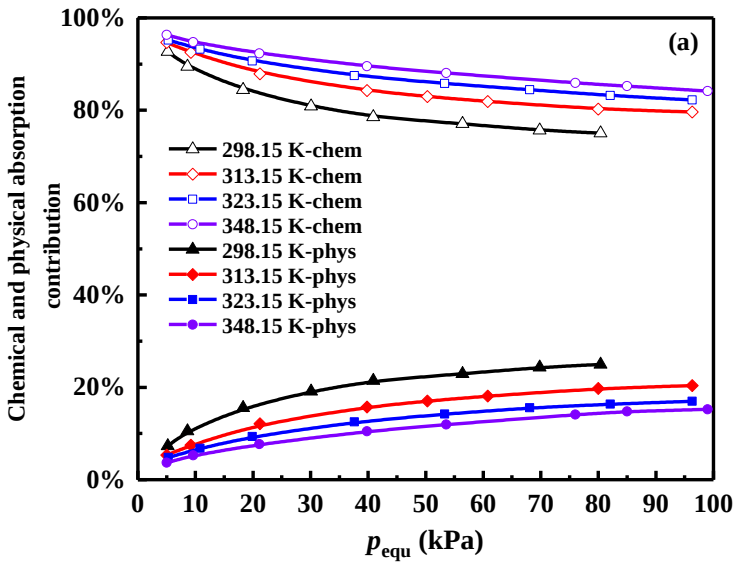

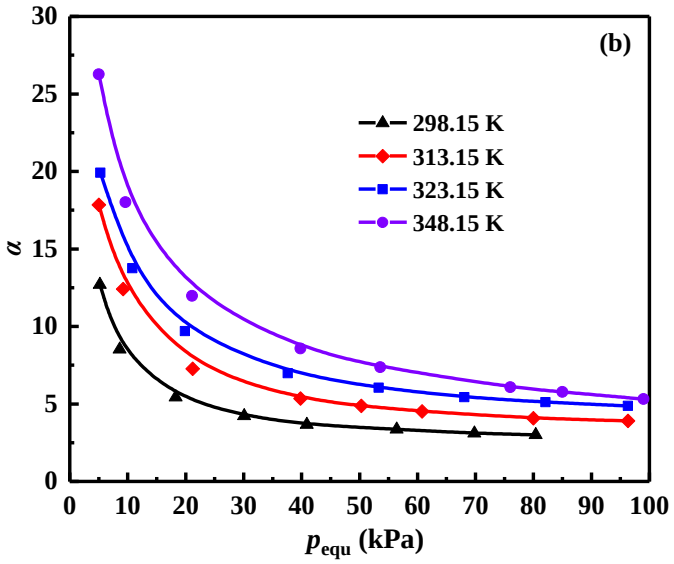

Fig. 7. The contribution of chemisorption and physisorption as functions of temperature and pressure. (a) Chemical and physical absorption contributions to CO_2 absorption capacity and (b) the ratio of chemisorption and physisorption (α). (Lines are fitted experiment data trend lines).

As shown in Fig. 7a, with the increase of pressure, the contribution of physisorption to absorption process increases whereas an opposite effect on the contribution of chemisorption is observed. With regard to temperature, it is found that the physisorption contribution is decreased at higher temperature, bringing about an increasing chemisorption contribution correspondingly. The effect of temperature and pressure on the physisorption and chemisorption contribution can also be reflected from Fig. 7b. An upward trend of α is witnessed with increasing the temperature, which is resulted from the less effect of temperature on C_{chem} compared with C_{phys}[30]. By contrast, a downward trend of α is experienced with increasing the pressure, which is caused by the gradually ascending difference between C_{phys} and C_{chem} caused by the approach of chemisorption equilibrium. Moreover, it is worth mentioning that in all the 32 studied entries, the α are higher than 3, that is to say, the molar factions of

chemisorption are more than 75%. This finding clearly demonstrates that [Emim][OAc] is favorable for CO_2 activation and conversion, which is in good agreement with previous studies that utilize this character [22].

3.4. Thermodynamic analysis

In the chemisorption by [Emim][OAc], the Emim−CO_2 adduct is the main chemical absorption product, which plays a key role in the absorption and release of gaseous CO_2 [28]. The stability constant of the Emim−CO_2 adduct ($K_{stability}$), which is important for evaluating the performance of chemical absorbents, is calculated as:

$$K_{stability} = \frac{c_{Emim\text{-}CO2} c_{CH3COOH}}{c_{[Emim][OAc]} c_{CO2}} \quad (24)$$

where c_A represents the concentration of compound A. Essentially, $K_{stability}$ is equivalent to the concentration-based chemical equilibrium constant and has been applied to the stability estimation of carbamates produced by CO_2 chemisorption in alkanolamines [28,46,47]. With the known C_{chem} and $C_{phys,}$ the expression of $K_{stability}$ can be rewritten as:

$$K_{stability} = \frac{C_{chem} C_{chem}}{(1 - C_{chem}) C_{phys}} \quad (25)$$

Table 3. The apparent Emim−CO_2 adduct stability constant ($K_{stability}$) in {[Emim][OAc] + CO_2} system.

T (K)	p_{equ} (kPa)	$K_{stability}$	T (K)	p_{equ} (kPa)	$K_{stability}$
298.15	5.2	2.68	313.15	5.0	2.21
298.15	8.6	2.03	313.15	9.2	1.97
298.15	18.3	1.54	313.15	21.2	1.50
298.15	30.1	1.34	313.15	39.8	1.40
298.15	40.9	1.23	313.15	50.3	1.40
298.15	56.4	1.22	313.15	60.8	1.40
298.15	69.8	1.16	313.15	80.0	1.34

298.15	80.4	1.15	313.15	96.3	1.32
323.15	5.3	1.81	348.15	5.0	1.42
323.15	10.8	1.74	348.15	9.6	1.28
323.15	19.9	1.55	348.15	21.1	1.24
323.15	37.6	1.45	348.15	39.8	1.18
323.15	53.3	1.41	348.15	53.6	1.15
323.15	68.1	1.36	348.15	76.0	1.07
323.15	82.1	1.34	348.15	85.0	1.06
323.15	96.3	1.31	348.15	99.0	1.01

As shown in Table 3, the $K_{stability}$ in the 32 studied entries vary in the range of 1.01 to 2.68, which indicates a certain stability of Emim−CO_2 adduct that can facilitate CO_2 conversion. Furthermore, $K_{stability}$ could also indicate the difficulty of desorption of the {[Emim][OAc] + CO_2} system. Comparing with the carbamate of the {MEA aqueous solutions + CO_2} system (e.g., $K_{stability}$ are 2100 and 775 at 293.15 K and 313.15 K, respectively) [46], $K_{stability}$ of the Emim−CO_2 adduct is much smaller, demonstrating that [Emim][OAc] is more favorable than MEA in CO_2 desorption cycles. This point has been proved by Li et al. [48], wherein [Emim][OAc] can obtain higher regeneration efficiency compared with MEA aqueous solution. Besides, $K_{stability}$ varies negatively with the temperature, implying that the chemisorption of CO_2 in [Emim][OAc] is an exothermic reaction. Similar with α, $K_{stability}$ decreases with the increasing equilibrium pressure at a certain temperature.

The quantification of physisorption contribution in the {[Emim][OAc] + CO_2} system allows the accurate estimation of the relevant thermodynamic properties. Fig. 8 depicts the physical solubility of CO_2 in [Emim][OAc] at the four different temperatures, which are found to be notably deviated from the Henry's law. To describe this physical solubility quantitatively, the temperature-dependent Krichevsky-Kasarnovsky (K-K) equation (Eq. (26)) is applied [49-51].

$$\ln\left(\frac{f_1^{\gamma}}{x_1}\right) = \ln H_{12} + \frac{V^{\infty} p_{\mathrm{equ}}}{RT} \tag{26}$$

where x stands for the solubility of the gas (1, i.e., CO_2) in the solvent (2, i.e., [Emim][OAc]); H_{12} represents the Henry's law constant for species 1 in 2. V^{∞} is the infinite dilution partial molar volume of the gas; p_{equ} refers to the CO_2 equilibrium partial pressure. By correlating H_{12}, other important thermodynamic properties namely the physisorption enthalpy (ΔH_{phys}), physisorption Gibbs free energy (ΔG_{phys}), and physisorption entropy (ΔS_{phys}) can be determined by:

$$\Delta H_{\mathrm{phys}} = -RT^2 \frac{\partial}{\partial T} \ln\left(\frac{H_{12}}{p^0}\right) \tag{27}$$

$$\Delta G_{\mathrm{phys}} = RT \ln\left(H_{12}/p^0\right) \tag{28}$$

$$\Delta S_{\mathrm{phys}} = \left(\Delta H_{\mathrm{phys}} - \Delta G_{\mathrm{phys}}\right)/T \tag{29}$$

where p^0 refers to the standard pressure of 100 kPa.

The fitting results of the temperature-dependent K-K equation are also shown in Fig. 8 and tabulated in detail in Table S3 (Supporting Information). It can be found that the K-K equation is highly accurate in correlating the physical solubility data of CO_2 in [Emim][OAc] with an absolute average relative deviations (AARD) of 1.1%. The thermodynamic properties correlated based on the physical CO_2 solubility are listed in Table 4. The strong interactions between CO_2 and OAc^- ions by forming a stable CO_2–anion associate can change molecular state of CO_2 dissolved in liquid phase [52], and thus the relationship between physical CO_2 solubilities and pressures leads to deviate from Henry's law at low pressures. As seen, H_{12} increases with temperature (from 367.9 kPa at 298.15 K to 2547.6 kPa at 348.15 K), and V^{∞} falls with less free volume available to accommodate CO_2 in [Emim][OAc] when the temperature rises, which is consistent with the finding from the obtained solubility. The positive values of

ΔG_{phys} show that the absorption of CO_2 into [Emim][OAc] is a nonspontaneous process. It increases with the increase of temperature, indicating that the degree of non-spontaneity of the system increases with temperature, which is not conducive to the CO_2 physisorption [36].

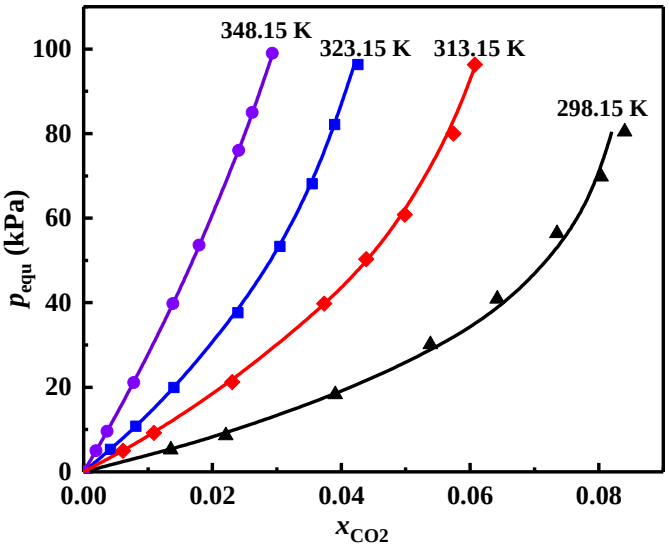

Fig. 8. Physical solubility of CO_2 in [Emim][OAc] at ▲ 298.15 K; ◆ 313.15 K; ■ 323.15 K; ● 348.15 K. Markers show the experimental data, and lines show the fitting results from K-K equation.

The values of ΔH_{phys} are all negative, suggesting that the physisorption of CO_2 in [Emim][OAc] is exothermic. Furthermore, ΔH_{phys} also reflects the physical interactions of CO_2 with [Emim][OAc], a more negative ΔH_{phys} indicates stronger interactions and thus a larger physical absorption capacity [51]. As seen, the calculated ΔH_{phys} is more negative at lower temperature (-44.24 $kJ \cdot mol^{-1}$ at 298.15 K vs -22.79 $kJ \cdot mol^{-1}$ at 348.15 K). In other words, the interaction between CO_2 and [Emim][OAc] decreases with rising temperature, resulting in the decrease in physical solubility. Besides, the negative ΔS_{phys} demonstrates that the higher ordering degree of {[Emim][OAc] + CO_2} system from a molecular level after CO_2 absorption [36].

Table 4. Thermodynamic properties of physisorption in {[Emim][OAc] + CO_2} system.

T (K)	H_{12} (kPa)	V^{∞} ($L \cdot mol^{-1}$)	ΔG_{phys} ($kJ \cdot mol^{-1}$)	ΔH_{phys} ($kJ \cdot mol^{-1}$)	ΔS_{phys} ($J \cdot mol^{-1} \cdot K^{-1}$)
298.15	367.9	36.18	3.23	-44.24	-159.2
313.15	790.8	20.84	5.38	-37.08	-135.6
323.15	1234.7	18.96	6.75	-32.68	-122.0
348.15	2547.6	8.39	9.37	-22.79	-92.4

4. Conclusion

An experimental approach for straightforwardly quantifying the chemisorption and physisorption contribution in chemisorptive absorbent system is proposed and exemplified by the CO_2 capture with [Emim][OAc]. A set of 32 data points of the total CO_2 solubility in [Emim][OAc] is measured by the pressure drop method, covering the low pressure range below 100 kPa at four different temperatures. The chemisorption contribution to the total CO_2 solubility is accurately determined by the qNMR spectroscopy, and subtracting this part from the total CO_2 solubility gives the physisorption contribution. Based on the quantitatively distinguished chemical and physical solubility of CO_2 in this IL, the stability constant of the chemisorptive product (i.e., Emim−CO_2 adduct) is found to reach a good trade-off between adduct stability and the desorption easiness; the physisorption related thermodynamic properties including the Henry's law constant, the infinite dilution partial molar volume of gas, the physisorption enthalpy, Gibbs free energy, and entropy are rationally derived and interpreted. The illustrated approach in this work could be widely extended for unveiling solubility behaviors of gas in simultaneous chemisorption and physisorption

processes.

Conflicts of interest

The authors declare that there are no conflicts of interest.

Acknowledgements

The financial support from National Natural Science Foundation of China (21861132019 and 21576081) and Natural Science Foundation of Shanghai (19ZR1412500) is greatly acknowledged.

Nomenclature

p_{ini} = initial partial pressure of CO_2, kPa

p_{equ} = equilibrium partial pressure of CO_2, kPa

V_{sys} = volume of absorption system, mL

n_{CO2} = solubility of CO_2 in [Emim][OAc], mol

C_{CO2} = total absorption capacity of CO_2, mol CO_2·mol^{-1} IL

C_{phys} = physisorption capacity of CO_2, mol CO_2·mol^{-1} IL

C_{chem} = chemisorption capacity of CO_2, mol CO_2·mol^{-1} IL

x_{CO2} = molar fraction of CO_2

U = expanded uncertainty

$\bar{x}$ = themean of all data points

u_c = combined uncertainty

I = integral area

Z = number of components or data points

N = number of excited atoms

$d1$ = relaxation delay, s

Ns = number of scans

α = ratio of chemisorption to physisorption

$K_{stability}$ = apparent stability constant of Emim−CO_2 adduct

V^{∞} = infinite dilution partial molar volume, L·mol^{-1}

H_{12} = Henry's law constant, kPa

ΔH_{phys} = physisorption enthalpy, kJ·mol^{-1}

ΔG_{phys} = physisorption Gibbs free energy, kJ·mol^{-1}

ΔS_{phys} = physisorption entropy, J·mol^{-1}·K^{-1}

References

[1] S. Sarmad, J.P. Mikkola, X.Y. Ji, Carbon dioxide capture with ionic liquids and deep eutectic solvents: a new generation of sorbents, ChemSusChem 10 (2017) 324–352.

[2] Y.J. Huang, G.K. Cui, Y.L. Zhao, H.Y. Wang, Z.Y. Li, S. Dai, J.J. Wang, Preorganization and cooperation for highly efficient and reversible capture of low-concentration CO_2 by ionic liquids, Angew. Chem. Int. Ed. 56 (2017) 13293–13297.

[3] J.W. Wang, Z. Song, H.Y. Cheng, L.F. Chen, L.Y. Dengd, Z.W. Qi, Multilevel screening of ionic liquid absorbents for simultaneous removal of CO_2 and H_2S from natural gas, Sep. Purif. Technol. 248 (2020) 117053.

[4] G.T. Rochelle, Amine scrubbing for CO_2 capture, Science 325 (2009) 1652–1654.

[5] S. Mukherjee, P. Kumar, A. Hosseini, A. Yang, P. Fennell, Comparative assessment of gasification based coal power plants with various CO_2 capture technologies producing electricity and hydrogen, Energy Fuel 28 (2014) 1028−1040.

[6] Y.J. Huang, G.K. Cui, H.Y. Wang, Z.Y. Li, J.J. Wang, Tuning ionic liquids with imide-based anions for highly efficient CO_2 capture through enhanced cooperations, J. CO_2 Util. 28 (2018) 299–305.

[7] G.T. Rochelle, Thermal degradation of amines for CO_2 capture, Curr. Opin. Chem. Eng. 1 (2012) 183–190.

[8] S.J. Zeng, X.P. Zhang, L. Bai, X.C. Zhang, H. Wang, J.J. Wang, D. Bao, M.D. Li, X.Y. Liu, S.J. Zhang, Ionic-liquid-based CO_2 capture systems: structure, interaction and process, Chem. Rev. 117 (2017) 9625–9673.

[9] Z.J. Huang, J. Uranga, S.L. Zhou, H. Jia, Z.F. Fei, Y.F. Wang, F. Bobbink, Q.H. Lu,

P.J. Dyson, Ionic liquid containing electron-rich, porous polyphosphazene nanoreactors catalyze the transformation of CO_2 to carbonates, J. Mater. Chem. A 6 (2018) 20916–20925.

[10] F. Karadas, M. Atilhan, S. Aparicio, Review on the use of ionic liquids (ILs) as alternative fluids for CO_2 capture and natural gas sweetening, Energy Fuel 24 (2010) 5817–5828.

[11] Z.G. Lei, C.N. Dai, B. Chen, Gas solubility in ionic liquids, Chem. Rev. 114 (2014) 1289–1326.

[12] W.L. Xu, J.Y. Zhang, N.N. Cheng, Z.L. Li, H.C. Lan, W.J. Jiang, H.L. Peng, K. Huang, J. Du, Dispersing aminopolycarboxylate ionic liquids in mesoporous organic polymer for highly efficient and improved carbon capture from dilute source, J. Mol. Liq. 338 (2021) 116653.

[13] M. Taheri, C.N. Dai, Z.G. Lei, CO_2 capture by methanol, ionic liquid, and their binary mixtures: experiments, modeling, and process simulation, AIChE J. 64 (2018) 2168–2180.

[14] J.N. Zhang, D.L. Peng, Z. Song, T. Zhou, H.Y. Cheng, L.F. Chen, Z.W. Qi, Multilevel screening of ionic liquid absorbents for simultaneous removal of CO_2 and H_2S from natural gas, Chem. Eng. Sci. 162 (2017) 355–363.

[15] C.M. Wang, X.Y. Luo, H.M. Luo, D.E. Jiang, H.R. Li, S. Dai, Tuning the basicity of ionic liquids for equimolar CO_2 capture, Angew. Chem. Int. Ed. 2011 (50) 4918–4922.

[16] J. Li, Z.D. Dai, M. Usmana, Z.W. Qi, L.Y. Deng, CO_2/H_2 separation by amino-acid ionic liquids with polyethylene glycol as co-solvent, Int. J. Greenh. Gas Control

45 (2016) 207–215.

[17] E.D. Bates, R.D. Mayton, I. Ntai, J.H. Davis, CO_2 capture by a task-specific ionic liquid, J. Am. Chem. Soc. 124 (2002) 926–927.

[18] P. Sharma, S.D. Park, K.T. Park, S.C. Nam, S.K. Jeong, Y.I. Yoon, I.H. Baek, Solubility of carbon dioxide in amine-functionalized ionic liquids: role of the anions, Chem. Eng. J. 193-194 (2012) 267–275.

[19] B.E. Gurkan, J.C.d.l. Fuente, E.M. Mindrup, L.E. Ficke, B.F. Goodrich, E.A. Price, W.F. Schneider, J.F. Brennecke, Equimolar CO_2 absorption by anion-functionalized ionic liquids, J. Am. Chem. Soc. 132 (2010) 2116–2117.

[20] A. Yokozeki, M.B. Shiflett, C.P. Junk, L.M. Grieco, T. Foo, Physical and chemical absorptions of carbon dioxide in room-temperature ionic liquids, J. Phys. Chem. B 112 (2008) 16654–16663.

[21] G. Gurau, H. Rodríguez, S.P. Kelley, P. Janiczek, R.S. Kalb, R.D. Rogers, Demonstration of chemisorption of carbon dioxide in 1,3-dialkylimidazolium acetate ionic liquids, Angew. Chem. Int. Ed. 50 (2011) 12024–12026.

[22] X.T. Hu, J.W. Wang, M.C. Mei, Z. Song, H.Y. Cheng, L.F. Chen, Z.W. Qi, Transformation of CO_2 incorporated in adducts of *N*-heterocyclic carbene into dialkyl carbonates under ambient conditions: an experimental and mechanistic study, Chem. Eng. J. 413 (2021) 127469.

[23] Z. Zhang, L. Zhang, L. He, W.L. Yuan, D. Xu, G.H. Tao, Is it always chemical when amino groups come across CO_2? Anion-anion-interaction-induced inhibition of chemical adsorption, J. Phys. Chem. B 123 (2019) 6536–6542.

[24] B.F. Goodrich, J.C. de la Fuente, B.E. Gurkan, D.J. Zadigian, E.A. Price, Y. Huang, J.F. Brennecke, Experimental measurements of amine-functionalized anion-tethered ionic liquids with carbon dioxide, Ind. Eng. Chem. Res. 50 (2011) 111–118.

[25] B.F. Goodrich, J.C. de la Fuente, B.E. Gurkan, Z.K. Lopez, E.A. Price, Y. Huang, J.F. Brennecke, Effect of water and temperature on absorption of CO_2 by amine-functionalized anion-tethered ionic liquids, J. Phys. Chem. B 115 (2011) 9140–9150.

[26] K. Mei, X. He, K.H. Chen, X.Y. Zhou, H.R. Li, C.M. Wang, Highly efficient CO_2 capture by imidazolium ionic liquids through a reduction in the formation of the carbene-CO_2 complex, Ind. Eng. Chem. Res. 56 (2017) 8066–8072.

[27] A.H. Tamboli, A.A. Chaugule, H. Kim, Highly selective and multifunctional chitosan/ionic liquids catalyst for conversion of CO_2 and methanol to dimethyl carbonates at mild reaction conditions, Fuel 166 (2016) 495–501.

[28] S. Wada, T. Kushida, H. Itagaki, T. Shibue, H. Kadowaki, J. Arakawa, Y. Furukawa, ^{13}C NMR study on carbamate hydrolysis reactions in aqueous amine/CO_2 solutions, Int. J. Greenh. Gas Control 104 (2021) 103175.

[29] F.D. Bobbink, W. Gruszka, M. Hulla, S. Das, P.J. Dyson, Synthesis of cyclic carbonates from diols and CO_2 catalyzed by carbenes, Chem. Commun. 52 (2016) 10787–10790.

[30] J. Blath, N. Deubler, T. Hirth, T. Schiestel, Chemisorption of carbon dioxide in imidazolium based ionic liquids with carboxylic anions, Chem. Eng. J. 181 (2012) 152–158.

[31] S. Bishnoi, G.T. Rochelle, Physical and chemical solubility of carbon dioxide in

aqueous methyldiethanolamine, Fluid Phase Equilib. 168 (2000) 241–258.

[32] B.E. Gurkan, T.R. Gohndrone, M.J. McCready, J.F. Brennecke, Reaction kinetics of CO_2 absorption in to phosphonium based anion-functionalized ionic liquids, Phys. Chem. Chem. Phys. 15 (2013) 7796–7811.

[33] K. Huang, Y.T. Wu, S. Dai, Sigmoid correlations for gas solubility and enthalpy change of chemical absorption of CO_2, Ind. Eng. Chem. Res. 54 (2015) 10126–10133.

[34] S.K. Bharti, R. Roy, Quantitative ^{1}H NMR spectroscopy, Trac-Trends Anal. Chem. 35 (2012) 5–26.

[35] J. Li, Y.M. Ye, L.F. Chen, Z.W. Qi, Solubilities of CO_2 in poly(ethylene glycols) from (303.15 to 333.15) K, J. Chem. Eng. Data 57 (2012) 610–616.

[36] J.W. Wang, H.Y. Cheng, Z. Song, L.F. Chen, L.Y. Deng, Z.W. Qi, Carbon dioxide solubility in phosphonium-based deep eutectic solvents: an experimental and molecular dynamics study, Ind. Eng. Chem. Res. 58 (2019) 17514–17523.

[37] H. Qin, Z. Song, H.Y. Cheng, L.Y. Deng, Z.W. Qi, Physical absorption of carbon dioxide in imidazole-PTSA based deep eutectic solvents, J. Mol. Liq. 326 (2021) 115292.

[38] M. Fevre, J. Pinaud, A. Leteneur, Y. Gnanou, J. Vignolle, D. Taton, K. Miqueu, J.M. Sotiropoulos, Imidazol(in)ium hydrogen carbonates as a genuine source of N-heterocyclic carbenes (NHCs): applications to the facile preparation of NHC metal complexes and to NHC-organocatalyzed molecular and macromolecular syntheses, J. Am. Chem. Soc. 134 (2012) 6776–6784.

[39] G.F. Pauli, B.U. Jaki, D.C. Lankin, Quantitative ^{1}H NMR: development and potential of a method for natural products analysis, J. Nat. Prod. 68 (2005) 133–

149.

[40] G.F. Pauli, B.U. Jaki, D.C. Lankin, A routine experimental protocol for qHNMR illustrated with taxol, J. Nat. Prod. 70 (2007) 589–595.

[41] F. Malz, H. Jancke, Validation of quantitative NMR, J. Pharm. Biomed. Anal. 38 (2005) 813–823.

[42] M. Kanakubo, T. Makino, T. Umecky, CO_2 solubility in and physical properties for ionic liquid mixtures of 1-butyl-3-methylimidazolium acetate and 1-butyl-3-methylimidazolium bis(trifluoromethanesulfonyl)amide, J. Mol. Liq. 217 (2016) 112–119.

[43] M.B. Shiflett, D.J. Kasprzak, C.P. Junk, A. Yokozeki, Phase behavior of {carbon dioxide + [bmim][Ac]} mixtures, J. Chem. Thermodynamics 40 (2008) 25–31.

[44] F.Y. Jou, A.E. Mather, Solubility of carbon dioxide in an aqueous mixture of methyldiethanolamine and *N*-methylpyrrolidone at elevated pressures. Fluid Phase Equilib. 228−229 (2005) 465−469.

[45] J. Li, L.F. Chen, Y.M. Ye, Z.W. Q, Solubility of CO_2 in the mixed solvent system of alkanolamines and poly(ethylene glycol) 200, J. Chem. Eng. Data 59 (2014) 1781–1787.

[46] J.P. Jakobsen, J. Krane, H.F. Svendsen, Liquid-phase composition determination in CO_2-H_2O-alkanolamine systems: an NMR study, Ind. Eng. Chem. Res. 44 (2005) 9894–9903.

[47] C. Perinu, B. Arstad, A.M. Bouzga, J.A. Svendsen, K.J. Jens, NMR-based carbamate decomposition constants of linear primary alkanolamines for CO_2 capture, Ind. Eng. Chem. Res. 53 (2014) 14571–14578.

[48] J. Li, C.J. You, L.F. Chen, Y.M. Ye, Z.W. Qi, K. Sundmacher, Dynamics of CO_2 absorption and desorption processes in alkanolamine with cosolvent polyethylene glycol, Ind. Eng. Chem. Res. 51 (2012) 12081–12088.

[49] B.D. Green, R.A. O'Brien, J.H. Davis, K.N. West, Ethane and ethylene solubility in an imidazolium-based lipidic ionic liquid, Ind. Eng. Chem. Res. 54 (2015) 5165–5171.

[50] A.H. Jalili, M. Safavi, C. Ghotbi, A. Mehdizadeh, M. Hosseini-Jenab, V. Taghikhani, Solubility of CO_2, H_2S, and their mixture in the ionic liquid 1-octyl-3-methylimidazolium bis(trifluoromethyl)sulfonylimide, J. Phys. Chem. B 116 (2012) 2758–2774.

[51] X.M. Zhang, X. Feng, H. Li, J. Peng, Y.T. Wu, X.B. Hu, Cyano-containing protic ionic liquids for highly selective absorption of SO_2 from CO_2: experimental study and theoretical analysis, Ind. Eng. Chem. Res. 55 (2016) 11012–11021.

[52] O. Hollóczki, D.S. Firaha, J. Friedrich, M. Brehm, R. Cybik, M. Wild, A. Stark, B. Kirchner, Carbene formation in ionic liquids: spontaneous, induced, or prohibited? J. Phys. Chem. B 117 (2013) 5898-5907.